A Wearable Self-powered System Based on Piezoelectric Energy Harvester

Zhenghong Chen
*q*us9bh@virginia.edu

Shan He
*k*fs4bm@virginia.edu

***Abstract*—This paper discusses the development and application of piezoelectric-based energy harvesters. Firstly, the design ideas and simulation results of the piezoelectric energy harvester arranged in the knee position are studied. Then, a self-powered system is designed based on piezoelectric energy harvesters. Using this self-powered system can be worn for a long time to detect motion. By simulating the test subjects for 7 days, the sustainability of the system was successfully ensured.**

***Index Terms*—Piezoelectric, Energy harvester, Self-powered, Wearable**

I. Introduction

A. Piezoelectric Energy Harvesters

Piezoelectric energy harvesters (PEHs) collect energy from the ambient environment to supply power to the self-powered systems by utilizing mechanical and vibration energy sources. PEHs are small, light, and have a high-power density, which makes them suitable to be implemented in wearable electronic devices. Jingjing Zhao proposed a show-embedded piezoelectric energy harvester that could provide an output power of around 1mW at the walking frequency of 1Hz. A shoe-mounted piezoelectric transducer made with PZT and PVDF materials was designed by Shenck. This energy harvester could produce on average 8.4mW in a 500-kΩ load. In 2017, Yang Kuang presented a sandwiched piezoelectric transducer that generated output power of about 2.5mW at a walking speed of 4.8km/h.

B. Full-Bridge Rectifier and Parallel-SSHI Rectifier

The energy harvested from transducers needs to be stored in batteries or supercapacitors, which requires a rectifier to transfer the AC voltage to DC voltage. The full-bridge diode rectifier (FBR) is a standard passive interface to extract energy from an AC source. However, during the process of charging and discharging capacitors, much energy is going to be lost. (Fig. 1a) In this project, we implemented the parallel-SSHI technique (synchronized switch harvesting on inductor) to improve the efficiency of the interface. [2] By controlling the switches, the resonant circuit is formed when the polarity of the current source changes, then the output voltage could be flipped quickly to reduce the power consumption. This process is shown in Fig. 1b.

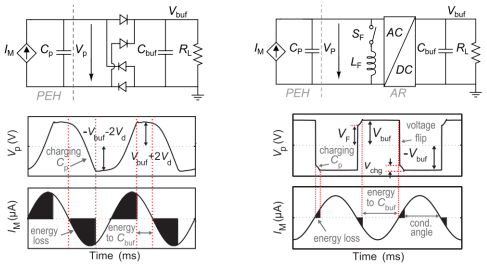

Fig. 1. The schematic of FBR and parallel-SSHI rectifier connected to a PEH and their operation waveform.

II. The model of the Piezoelectric Energy Harvesting System

A. The model of the bending beam-based PEH

In this project, we choose the lightweight piezoelectric bending beam-based energy harvester proposed by Fei Gao [1]. This energy harvester scavenges energy from human knee motion by bending the piezoelectric beam to power the body-worn electronics. The piezoelectrical material of this transducer is MFC (macro fiber composites). Compared with PZT, it is more flexible, and compared with PVDF, its power density is higher. By modeling this PEH, we get the plot of output voltage.

The process of modeling the bending beam-based PEH is demonstrated in Fig. 2. By citing the data of knee angles measured while walking [1], we could calculate the displacement of the end of the beam from the slider-crank mechanism model. Next, according to the bending beam model introduced in [1], we could get the relationship between the average strain and the displacement. Finally, we build up the piezoelectric transducer module to get the output voltage of the PEH. (Fig. 3)

B. The model of the Rectifiers

The circuit of the FBR is presented in Fig. 1. Because of the high impedance of the piezoelectric material MFC, we consider it as a current source. The simulation results of the output voltage and current of the piezoelectric energy harvester are presented in Fig. 4.

The circuit of the p-SSHI Rectifier is presented in Fig. 1. By controlling the switch closing at the time the polarity of the

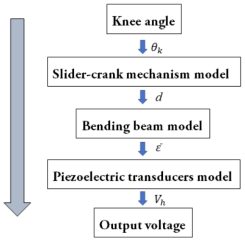

Fig. 2. The design flow of modeling the piezoelectric energy harvester.

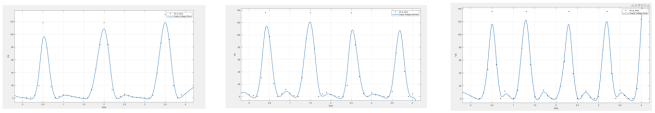

Fig. 3. The output voltage of PEH at different walking speeds

current source changed, we could build up an LF-Cp resonant circuit to get rid of the phase of charging and discharging Cp capacitor. Then the Vp could be quickly flipped and continue the energy extraction. The output waveform of the PEH when it connected to a p-SSHI interface is shown in Fig. 5.

The output power, the voltage of storing capacitors of two kinds of rectifiers are available in Table 1.

TABLE I
THE OUTPUT VOLTAGE AND POWER OF RECTIFIERS

Walking Speed	Voltage and Power			
	FBR Output Voltage of Store Capacitor (V)	*p-SSHI Output Voltage of Store Capacitor (V)*	*FBR Output Power (uW)*	*p-SSHI Output Power (uW)*
Slow	3.1	3.5	3.289	61.543
Normal	4.8	5.3	9.485	120.55
Fast (3.3 mH)	5.5	4.9	15.30	112.71
Fast (3.6 mH)	5.5	6.8	15.30	198.85

III. Trade-offs in Piezoelectric Energy Harvesting System

The first trade off in a PEH system is the area of the MFC transducer versus the comfort and economic cost. If we increase the area of the MFC material, we could harvest more power to supply loads. However, that also means the transducer would be more expensive. Moreover, people will feel uncomfortable if the transducer is too large to wear and may influence their motions.

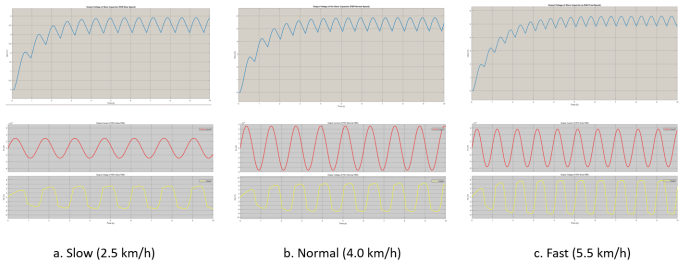

Fig. 4. The output and input voltage of the FBR when connencted to the PEH at different walking speeds

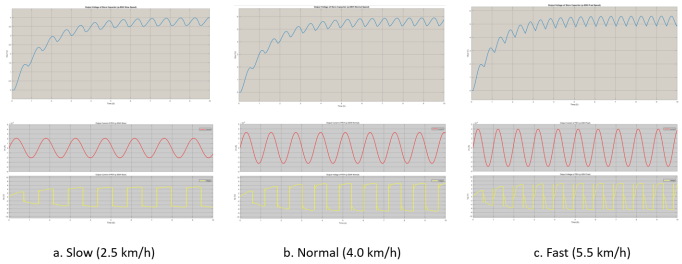

Fig. 5. The output and input voltage of the p-SSHI Rectifier when it connencted to the PEH at different walking speeds

The second trade off is the piezoelectric material that implemented to the transducers. The MFC is more flexible than PZT, but the power density of MFC is lower than PZT. When compared with PVDF, even though the power density of MFC is higher, its flexibility is not as good as PVDF.

The last trade off is that if we use the parallel-SSHI rectifier to extract energy from AC source, the efficiency is much higher than the standard full-bridge rectifier. However, the circuit would be more complex, and we need to design MMPT circuits to keep the high efficiency.

IV. System Block Diagram

For our design considerations, based on our completed energy harvesting and energy consumption models. We want to design with the structure in the System Block Diagram during operation.(Fig. 6) In terms of details, we selected products from various Volkswagen hardware manufacturers. The first is our microcontroller, based on the choice of low

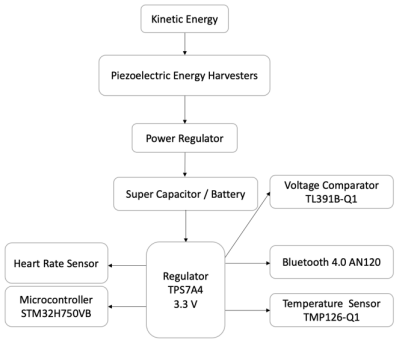

Fig. 6. Block Diagram

power consumption of the microcontroller, we decided to use the STM32H750VB. This is a microcontroller with low power mode, its working voltage is 3.3 V. In low-power mode, the STM32H750VB consumes 89.1 μW of operating power and 0.445 uW of static power. The Bluetooth low energy component is our main energy-consuming device. In our system, the duty cycle of the Bluetooth component is very low, but it also generates a lot of power consumption during operation. We choose the Bluetooth 4.0 AN120. The Bluetooth 4.0 AN120 uses the CC2590 front end and a CC2541 control

unit. We use the lowest power consumption in A mode, Voltage requirement is 3.3 V, Transmit Current is 27.5 mA, and Idle Current is 0.5 uA. Based on the Bluetooth device data throughput of 0.305 Mb/s, we estimate that we need 1s to complete a signal transmission. Then there are the sensor components used for data measurement, temperature sensor TMP126-Q1 and photoplethysmography heart rate sensor. The required Voltage of TMP126-Q1 is 3.3 V, Active Power is 547.4 uW, Idle Power is 38.2 uW. Heart rate sensor we chose a This is because the PPG can be tested more accurately, even if it consumes more power. We expect each test to take 5 s to complete, while its Voltage is 3.3 V, Active Power is 547.4 uW, and Idle Power is 38.2 uW, which are data including LED devices.Last is the voltage comparator TL391B-Q1 [4] and the Regulator TPS7A4 [5].Voltage comparator TL391B-Q1 is used to find the relationship betwwen the power storage and the work type. We hope to monitor the energy storage in real time to get the desired working state. The working voltage of TL391B-Q1 is 3.3 V and the working current is 2 uA. The Regulator TPS7A4 acts as a regulator between the balance energy storage element and the voltage supply. Our load systems are powered by 3.3 V, which allows us to reduce voltage regulation losses and improve efficiency. The input voltage range of TPS7A4 is 1.6 V - 6.0 V, the output voltage range is 0.8 V - 5.5 V, and the operating current is 6.5 uA.

V. System Simulation

We want our process management to be based on the results of different activity states. For example, running will generate more energy, and we can use the load at a higher frequency to obtain more and more accurate data. From our simulated component usage frequency, we can perform a duty cycle calculation. A table is drawn based on our calculations of the energy produced by the piezoelectric energy harvester and the energy consumed by the load.

TABLE II
Components Running Duty Cycle and Power

Components	Activity Type				
	A [a]	***B*** [b]	***C*** [c]	***D*** [d]	***E*** [e]
Microcontroller	0.0014	0.0042	0.0083	0.0168	0.042
Bluetooth	0	0.0001	0.0003	0.0006	
Temperature Sensor	0.00000167			0.00000333	
PPG HR Sensor	0.0014	0.0042	0.0083	0.0168	0.042
Step Range / Min	0	1-40	41-80	81-110	110..
EH Power(uW) [f]	0	379.92	535.14	871.44	1169.7
EC Power(uW) [g]	38	54	78	103	267

[a] Activity type A is rest.
[b] Activity type B is Light Activity.
[c] Activity type C is Walk.
[d] Activity type D is Fast Walk.
[e] Activity type E is Run.
[f] Power of energy harvester, calculate for each step.
[g] Power of energy energy consumption components.

By adjusting the duty cycle, we developed a work schedule. In each work plan, we hope to maintain a relatively stable accumulation of energy. Use different programs for different sports. I think it's more accurate to measure at high duty cycles. We looked for a detailed activity log [3]. In this record, we can clearly observe the detailed action plan of the recorded person for a week. This is an accurate dataset, it's down to the minute. Based on the previous values, we can judge the movement state of the recorded person per minute through the movement situation.(Fig. 7) Then we can draw the output power curve. Different sports have different energy harvesting intensity, this graph is different from the step distribution graph. This is because different states mean different bending properties, not just the number of steps. With 7 days of total energy harvesting (Fig. 8), we can derive the following total energy by comparing the power of harvested energy at different times. We can see that the energy harvesting is fast and slow. Comparing the energy harvesting power at different times, it is not difficult to see that the energy harvesting speed is fast during the day because it is in motion. Energy harvesting during the day is also fast and slow. This is because people are in different states of motion.

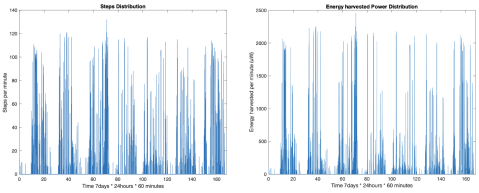

Fig. 7. 7 Days Activity Step and Power Distribution

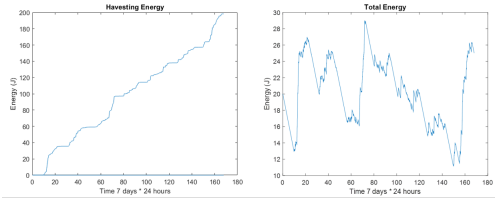

Fig. 8. 7 Days Activity Energy Change

Conclusion

This article discusses the development and application of piezoelectric-based energy harvesters. Based on the principle of piezoelectric energy harvesting, we arranged a piezoelectric energy harvester on the knee. Our design ideas and simulation results demonstrate that we can use piezoelectric energy harvesters as energy sources for self-powered systems. We adjust the duty cycle of each load to ensure that the self-powered system can be worn for long periods of time to detect motion. Finally, we obtained the 7-day power and energy changes through simulation, which successfully ensured the sustainability of the system.

References

[1] F. Gao, G. Liu, X. Fu, L. Li and W. -H. Liao, "Lightweight Piezoelectric Bending Beam-based Energy Harvester for Capturing Energy from

Human Knee Motion," in IEEE/ASME Transactions on Mechatronics, doi: 10.1109/TMECH.2021.3098719.

[2] D. A. Sanchez, J. Leicht, F. Hagedorn, E. Jodka, E. Fazel and Y. Manoli, "A Parallel-SSHI Rectifier for Piezoelectric Energy Harvesting of Periodic and Shock Excitations," in IEEE Journal of Solid-State Circuits, vol. 51, no. 12, pp. 2867-2879, Dec. 2016, doi: 10.1109/JSSC.2016.2615008.

[3] Lee, J., Jang, D.-H., Park, S., amp; Cho, S. H. (2018). A low-power photoplethysmogram-based heart rate sensor using Heartbeat Locked Loop. IEEE Transactions on Biomedical Circuits and Systems, 12(6), 1220–1229. https://doi.org/10.1109/tbcas.2018.2876671

[4] TPS7A43. TPS7A43 data sheet, product information and support — TI.com. (n.d.). Retrieved May 2, 2022, from https://www.ti.com/product/TPS7A43?keyMatch=amp;tisearch=search-everythingamp;usecase=partmatches

[5] Example data sets. (n.d.). Retrieved May 2, 2022, from https://www.fitabase.com/resources/knowledge-base/exporting-data/example-data-sets/